Analyzing Ballistic Trajectory Characteristics through MATLAB Simulation: A Computational Approach

[1] Er. Meemansa Mishra

[1] Department of Mechanical Engineering, I. K. Gujral Punjab Technical University, Main Campus, Kapurthala (Punjab), India
Corresponding Author Email: [1] meemansamishra11@gmail.com

Abstract— Unexpected air and marine attacks pose an increasing danger to security forces globally. For the sake of defensive systems readiness, it is essential to accurately anticipate trajectory elements for rockets and gun-type weapons, such as flight time and distance of impact. The evaluation and forecasting of ballistic trajectories by computational techniques have become possible because of recent developments in modeling technique, particularly MATLAB. Previous techniques required lengthy and costly field testing. The primary objective of the current paper is to use MATLAB to create a simulation framework that can precisely forecast the trajectory components of spin-stabilized flat-head mortar projectile and 130 mm rounds of artillery with explosives. Moreover, to calculate the motion of the projectile coefficients for an accurate trajectory estimate, the Runge-Kutta method is used in MATLAB. Furthermore, the MATLAB's plotting features are used to visualize the model of simulation and it is verified by data from experiments or analytical responses. In order to increase the consistency of predicted and experimental results, the investigation additionally examines the impact of taking Mach number into account while adjusting drag coefficient. The outcomes show the simulation's correctness and validate the mathematical framework and modeling methodology. This study emphasizes the significance of addressing shifting flow patterns by taking into consideration of the drag coefficient's non-constant character. The study emphasizes MATLAB's usefulness as a computational tool for studying ballistic trajectories and boosting defensive system readiness.

Keywords: Ballistic Trajectory; MATLAB; Runge-Kutta method; computational tool; mortar projectiles; rockets and gun-type weapons.

I. INTRODUCTION

Ballistic trajectory simulation plays a crucial role in various defense applications, offering a range of valuable uses. As an essential component of the Ministry of Defense, Government of India, the Defense Research and Development Organization (DRDO) assumes a pivotal role in advancing India's defense capabilities. With an extensive network of over 50 laboratories, establishments, and centers nationwide, DRDO brings together a diverse workforce of scientists, engineers, technicians, and support staff that work together to tackle difficult problems and present ground-breaking solutions. The following study delves into the subject of ballistic trajectory simulation, drawing insights from two distinct papers authored by DRDO scientists. The calculation of both static and dynamic parameters for missile trajectory and stability prediction is a fundamental area of aerodynamic study [1].Nevertheless, the reach of the weapon is vital throughout warfare because long-range devices offer the chance to launch an assault with fewer risks than short-range devices. At this point, several ranging enhancement and optimization researches have currently been carried out [2]. Although some studies concentrated on trajectory optimization, others concentrated on propeller conception optimization and aerodynamics form optimization. Corresponding to this, advances in technology may soon make it feasible to increase the reach of antiquated kinetic weapons with the aid of novel launching designs like magnetic or projectile capabilities. These missiles will give the ammunition a starting expulsion speed throughout launching that will further increase its range.

Consequently, a typical spin-stabilized flat-head ordnance bullet verification shoot is mathematically modeled using the reduced point-mass/simple component trajectory framework. In addition to problems with the projectile's dimensions and form as well as the complicated nature of air opposition, it is difficult to forecast its course with precision using mathematics [3]. The projectile's equations that govern the motion have been slightly modified for the sake of calculations and it is presumed that the shot is a molecule with only gravity and drag operating on it. Thus, each time step's associated vertical and horizontal elements of the projectile's speed and location have been estimated as well as the vertical and horizontal accelerations brought on by those forces. Moreover, the simulation was started with the starting parameters and speeds. Regarding exterior ballistics, the coefficient of drag is a crucial variable. A 130 mm ordnance round may travel up to 90.7 km in empty space with a muzzle speed of 943 m/s, however with the presence of air, that distance drops to 24 km [4]. As a result, the value of the coefficient of drag, which greatly relies on the projectile's tip form in its state of span and is quite important. The two types

of projectiles that are being taken into consideration here are the 130 mm wrap with recovering cap and the 130 mm wrap with fuze. Moreover, it is difficult to predict the trajectory components without access to the 130 mm shell's range tables (RTs). Ballistics is a branch of physics that studies the trajectory of projectiles. The English word "ballistics" was derived from the Latin phrase "ballista," which referred to a primitive contraption employed for launching javelins such as Internal, external and terminal ballistics respectively [5]. Regarding the development and evaluation of munitions as well as to comprehend the precision and efficacy of weapons, interior trajectory is crucial [6]. The investigation of a projectile's movement from the time it exits a gun's barrel till it lands on its intended location is known as external trajectory. This involves things like the projectile's path, speed and the aerodynamic characteristics. The development of exterior ballistics as they perceive it currently as a separate field of the mechanics of rigid objects travelling beneath the influence of gravity and aerodynamic force and is significant for firing from afar as well as for the development and testing of missiles with ballistic properties [7].

Consequently, the analysis of a projectile's behavior after impact is known as terminal ballistics. This encompasses the mechanisms of entry, impacts beneath armory, the distribution and toxicity of fragmentation mist, explosion overpressure, nonlethal impacts and the impact on tissue that is alive. Because of the increased interest in non-lethal weapons, this final subject becomes more and more important [8]. Typically, intercepting trajectory calculations are done offsite employing an expression of a two-point boundary-value issue. For obtaining the starting point trajectories, optimization methods are typically required [9]. Furthermore, one can employ a variety of techniques to determine the ideal intercepting site, including meta heuristic using traditional vibrational computation. Moreover, the process for employing key frames and checkpoints to create the quad rotor's ideal path. Additionally, there is a technique for controlling quad rotor trajectories in three directions that can meet specifications for roles, velocity, rising speeds and information inputs [10]. Therefore, the directions are perfect for the cap price operations that are obtained from the square root of the snapping norm. Such price capabilities are important because the information elements are exponentially connected to the status.

Key Contributions

The contributions can be further organized down into the following considerations:

- The project aims to develop a mathematical model using a simplified point-mass approach to mimic several aspects of a spin-stabilized flat-head ordnance bullet proof shot's trajectories.
- Numerical methods will be employed to accurately approximate the projectile's trajectory, considering

realistic parameters such as air resistance, wind speed and direction, altitude, and other relevant factors.
- Then, to visualize the simulated trajectory in a graphical format MATLAB's plotting capabilities will be utilized to generate plots that display the trajectory path.
- The simulation will be validated by comparing the results with known analytical solutions or experimental data.
- Finally, the findings will be documented and presented in a clear and concise manner.

The remaining of this study is divided into the resulting sections as follows: Section 2 exposes the relevant works are done from a thorough analysis. The ballistic theory and principles are explored in Section 3. Under Section 4, the outcomes of the experiment is reviewed and provided exactly. Section 5 is the conclusion of the paper.

II. RELATED WORKS

Jahangir et al.[11] revealed in his paper that, the primary goal of creating the source code was to improve students' both quantitative and qualitative comprehension of the complex elements (such as drag) controlling the movement of projectiles that are typically not covered in traditional texts. The researcher also says that, many students still struggle to understand the basics of movement of projectiles, particularly in a viscosity media. Moreover, students at both the undergraduate and graduate levels were presented with a method to demonstrate the movement of projectiles using MATLAB modeling. Hence, the pupils' exposure to certain sophisticated MATLAB capabilities is still an additional benefit of employing this method. The weakness of this study is movement with inaccuracy that is smaller than 10^{-6}. The acquired results consequently suggested that the MATLAB modeling of this study effectively offered a variety of possibilities for analyzing the trajectory of the projectile as an advantage. In 1870, the first known moving device was discovered said by Koushik et al.[12]. The ankle motion of a moving machine is a vital component that can have a big impact on how effective the machine is at stepping. After that time, scientists have worked to advance the machinery behind moving robotics. Nevertheless, numerous mobility devices that were developed in earlier times are mentioned in mythology. This study examines different leg returning trajectories that may deliver longer steps while using fewer calories. It is carried out via statistical analysis and experiments in programs like MSC Adams and Solid Works are used to verify it. Moreover, the two dimensions of mobility in a leg's kinematics and dynamic evaluation are also covered in this work utilizing mathematical techniques in MATLAB and simulation software in MSC Adams is used to confirm the findings. Even so, it was difficult to make significant advances in this area due to the intricacy of moving technique and its poor effectiveness. It is now much

easier to identify remedies for challenging mechanical problems due to advancements in computational capacity.

Głębocki and Jacewicz [13] disclosed in his paper that, in order to design missile direction, a wide range of potential travel situations with distinct system characteristics must be taken into account. In order to minimize bullet scattering and collateral harm, the Monte-Carlo parameterized research for a 160 mm ballistic launch outfitted with a total of 34 tiny, solid-fueled transverse rockets placed behind the center of gravity was analyzed in this work. The impact of different variables on the resultant precision at various launching altitude orientations was examined using a six-dimension freedom-based mathematical framework constructed in MATLAB/Simulink. Moreover, to implement trajectory sculpting capabilities, enhanced impacting site predictive assistance was used in the airborne trajectories' falling section. Moreover, the uniqueness of this study resides in its ability to change the trajectory's form during the last stage solely by means of diagonal rockets. The study of innovative smart control systems has both great academic and operational importance and it is important to note that this new rocket management technique heavily relies on exterior weaponry said by Xu, Zhijun Wang, and Dong [14]. Nonetheless, modern conflict tactics require pinpoint attacks on adversary military installations with the least amount of incidental harm to populations and infrastructure that is used by civilians. This is necessitated by the continual creation of weaponry and military supplies. In addition to disturbance variables like fabrication/mismatch mistakes, beginning orientation and/or speed issues and random air impact, traditional missiles like grenades and explosives have a low chance of hitting their target. And this research's downside is thought to be these mistakes. Moreover, various methods for strengthening the construction of ammunition or weapons are used to increase firing distribution and lessen the impact of the aforementioned interfering elements, but their efficacy lags below the tactical demands in contemporary combat.

Moshtaghi Yazdani and Olyaei [15] said in his paper that, because of the numerous advantages , electrostatic rockets have recently piqued the interest of numerous academics and the militaries of several major nations are investing heavily in this type of weaponry. Nonetheless, numerous studies on various train weapon numbers have been conducted over the past few years. The magnetic rail gun's shot route and optimization are discussed in this study. The comparable circuit of the rail gun is retrieved from the circuit's model, which is utilized to imitate and optimize the electromagnetic rail gun. The electrostatic rail gun's bullet track and output from MATLAB's simulations of it have been examined via the ballistic route formulas and simulations. The fundamental benefit of the utilized models is that, because of their fast velocity, they may be applied in sensitive and optimization issues. According to the findings, losses and expenses are significantly decreased for the exact same goals, money as

well as energy wastage is avoided. An empirical measure of a rocket system's precision is called the circular error probability (CEP) parameter in the field of missile physics revealed by El-Hakem Hegazy et al.[16]. A missile that is ballistic may deviate from its optimum motion due to a variety of fault factors, which changes the needed CEP. The issues with strategic missile distribution brought on by INS mistakes are covered in this paper. The correct approaches are typically used to measure and adjust INS stochastic faults. INS unpredictable mistakes can actually be modeled and examined. Employing a ballistic aircraft trajectories model with six angles of independence, a specific rocket is carefully examined in this investigation.

Jacewicz et al.[17] disclosed in his paper that, an ordnance projectile's utility and efficacy are greatly influenced by identifying and reducing the effect's spot distribution. It is crucial to consider all potential outcomes, figure out and measure the distribution of potential places to land because of the shortcomings in the simulation of the trajectory associated with such items, unresolved reductions and uncertainty in the parameters of the model. The evaluation of the effect of spot dispersal minimization utilizing horizontal corrective rockets is presented in the paper. Using MATLAB/Simulink 2020b, a standard missile mathematics and simulation framework was developed. The effect on site deviation is significantly decreased when control techniques are used according to the outcomes. The foundation of kinetic software for computers is bullet trajectory analysis and modeling, which is crucial to understanding how weapons and bullets operate under different combat scenarios said by Rabbath and Corriveau [18]. An accurate estimate of the biomechanics is needed in order to create a computerized representation of bullet flight that is both efficient and accurate. The ballistic algorithm's aerodynamics parameters ought to be modeled as a set of individually quadratic derivatives of a Mach number that, in ideal conditions, satisfy the criteria as follows: they are constant, distinguishable more than once, and operate to a low degree. The procedures required to create these individually polynomial equations are described in the article along with resources that are easily accessible. Piecewise Cubic Hermite Interpolating Polynomial (PCHIP), a cubic spline and piecewise linear equations as well as their variants are then compared as the potential fit of curves approaches for estimating the aerodynamic appearances of a general tiny weapon missile. The primary flaw in this research is that whenever the PPF is used on powerful machines with the representation of numerical calculations performed with a fairly substantial number of bits of information there is no appreciable cutoff or wrapping mistake. Stearns and Moddel [19] revealed that in thermal rectennas, geometrical diodes, which are horizontal circuits with asymmetric patterns that offer electromagnetic imbalance, have shown high-energy inversion. These gadgets work through kinetic or quasi-ballistic transportation, in which the gadget's architecture

affects its mobility parameters. The consequences of particle velocity reduction are not taken into account by typical approaches for estimating device efficiency, which assume that electrons are completely linear. Considering the mean-free-path duration being lower than the crucial gadget parameters, the researchers describe a particle-in-cell Monte Carlo simulation technique that enables the forecasting of the current-voltage properties of geometrical transistors functioning quasi-ballistically. Moreover, the researchers discover that arbitrary big mean-free-path length are not preferred because the present inversion capacity of a specific shape is enhanced for a particular mean-free-path length. These findings open up a fresh perspective on geometrical impacts in the quasi-ballistic domain and demonstrate how the carrier's mean-free-path length and devices parameters can be changed to improve device efficiency.

III. BALLISTICS THEORY AND PRINCIPLES

Projectile motion is the subject of the science known as ballistics. The Latin word "ballista" refers to a prehistoric device used to launch javelins, from whence the English word "ballistics" was formed. Modern authors break the topic down into three categories. They are Internal ballistics, External ballistics and Terminal ballistics [20].

3.1 Internal Ballistics, Exterior Ballistics and Terminal Ballistics:

The investigation of the occurrences and procedures that take place inside a gun or other projectile-firing mechanism from the time that the propellant is lit through the bullet leaves the chamber is known as internal ballistics [21].. It is the study of the behavior of a projectile while it is still inside the firearm, including the ignition of the propellant, the expansion of gases, and the movement of the missile down the barrel. It is significant for understanding the accuracy and performance of firearms and for the design and testing of ammunition. Exterior Ballistics deals with the projectile's atmospheric flight. The investigation of bullet flight through a weapon's base to the destination is known as external ballistics. As soon as interior trajectory is over, exterior ballistics begins. Moreover, interior trajectory is only concerned with events that take place within the gun's chamber [22]. For computing trajectory elements, a number of trajectory models, each with a different level of complexity, have been created, including point mass model (PM), modified point mass model (MPM), six degrees of freedom models (6 DOFs). Terminal Ballistics describes the projectile's target contact action. A branch of ballistics called endpoint ballistics, commonly referred to as wound ballistics that examines the behavior and results of a missile as it strikes and imparts power to an object. Fig. (1) shows the diagram of the elements of ballistic trajectory
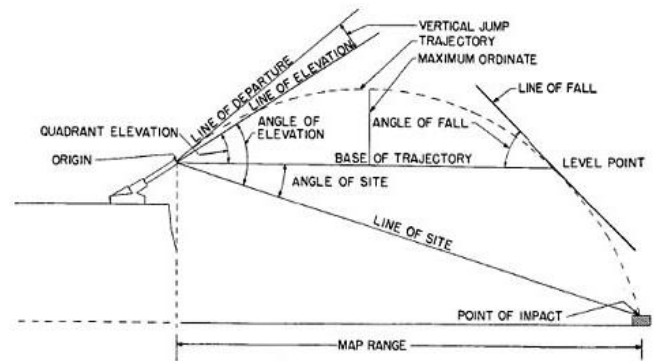

Figure 1: Elements of a ballistic trajectory [23]

3.1.1 Point Mass Model (PM)

In the field of trajectory computing, the traditional approach is based on the concept of point mass trajectory as exact mathematical prediction of the trajectory is challenging due to issues in the missile shape and size as well as the intricate nature resistance due to air .

- This approach primarily focuses on two main forces acting on a missile, drag and gravity.
- While the gravitational acceleration is well-known and constant, the calculation of drag involves coefficients that can vary based on the Mach number and differ for different types of trajectories.
- The point mass model undertakes that the entire mass of the projectile is concentrated at a single point, thus, its size and rotational effects are neglected.
- It simplifies the analysis by considering only the linear motion of the projectile and ignores any aerodynamic forces acting on different parts of the projectile's surface.

3.1.2 Modified Point Mass Model (MPM)

The modified point mass model goes beyond the simplistic representation of the projectile as a point mass. It takes into account the shape, size, and rotational effects of the projectile. It considers the aerodynamic forces acting on different parts of the projectile's surface due to its shape, spin, and yaw. It considers the drag force caused by the projectile's shape and the spin-induced lift and yaw forces. Pitch is the rotational motion of a projectile about its lateral axis, a hypothetical line passing through it horizontally is its center of gravity. Roll is the rotational movement of a projectile about its longitudinal axis, which is an imaginary line through the center of gravity of the projectile from snout to tail [24]. It describes the projectile's rotating motion around this axis. Yaw is the rotational movement of a projectile around its vertical axis, which is an imaginary line through the center of gravity of the projectile from top to bottom.

3.1.3 6 DOF Model and Motions

A more advanced and comprehensive approach that considers all six degrees of freedom: three linear (surge,

sway, heave) and three rotational (roll, pitch, yaw). It takes into account the projectile's linear and angular velocities, mass distribution, aerodynamic forces (drag, lift, and side forces), and gravity. The 6-DOF model offers a precision compromise between range and maximum height, improving efficiency. While accurate ranges may lead to less accurate maximum height results, and vice versa, the maximum relative errors are significantly smaller compared to other models. However, NATO recommends the Modified Point Mass Trajectory Model (MPMTM) as a basic alternative to the 6DOF model for live-fire situations as the commonly used 6DOF model, based on classical mechanics principles, is time-consuming and impractical. Both the MPM and 6-DOF models consider the transverse motion of the projectile, resulting in 3-D trajectories even in the absence of transverse wind. These models provide more accurate measurements and predictions of the projectile's behaviour. Thus, the PM model is the simplest, but it has a limitation in that it assumes a plane trajectory and neglects any lateral deviation of the projectile. Fig. (2) shows the diagrammatic representation of 6 DOF motions.

- The 6-DOF model has the best predictive capability among the three models, covering a wide range of possible trajectories with elevation angles up to 73-deg.

- Its theoretical development is most comprehensive, making it useful for understanding projectile dynamics and accurately predicting transverse motion.
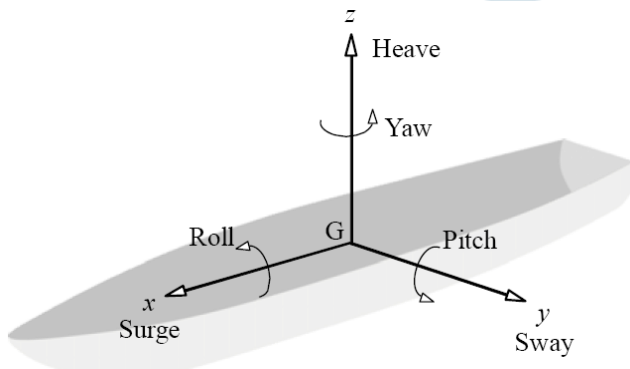

Figure 2: 6 DOF Motions [24]

3.2 Stabilization Techniques used in Ballistic Projectiles

3.2.1 Gyroscopic stability: Spin Stabilization and Aerodynamic Stability: Fin Stabilization

Gyroscopic stability is achieved by giving a projectile a spin around its longitudinal axis, creating a gyroscopic effect that causes it to resist changes in its orientation or angular momentum. The resistance to changes in orientation helps stabilize the projectile's flight and maintain its intended trajectory. Spin-stabilized projectiles use rifling or spiral grooves in the barrel of a firearm to impart a spin, which is maintained as the projectile exits the barrel. This gyroscopic force acts perpendicular to the spin axis and creates a

stabilizing torque that counteracts any disturbances or forces affecting the bullet when it is in flight. Aerodynamic stability relies on aerodynamic services substitute on the missile to maintain stability and its diagram is shown in Fig. 3(a). Fins, or control surfaces, are attached to the projectile to generate aerodynamic forces that stabilize its flight. The shape and arrangement of the fins are designed to create a stabilizing force that resists deviations or disturbances, keeping the projectile oriented along its intended flight path. The COP of a fin-stabilized projectile is located near the centre of the fins, and the aerodynamic forces acting on the fins cause a torque around the centre of gravity (CG). This torque aligns the projectile's longitudinal axis with its velocity vector, which is essential for stability. If the COP is located behind the CG, the torque produced by the aerodynamic forces tends to restore the projectile to its stable orientation. This is known as positive stability, where the projectile returns to its desired position when perturbed. Fin stabilization is commonly used in projectiles such as rockets, guided missiles, and certain artillery shells and its diagram is shown in Fig. 3(b).
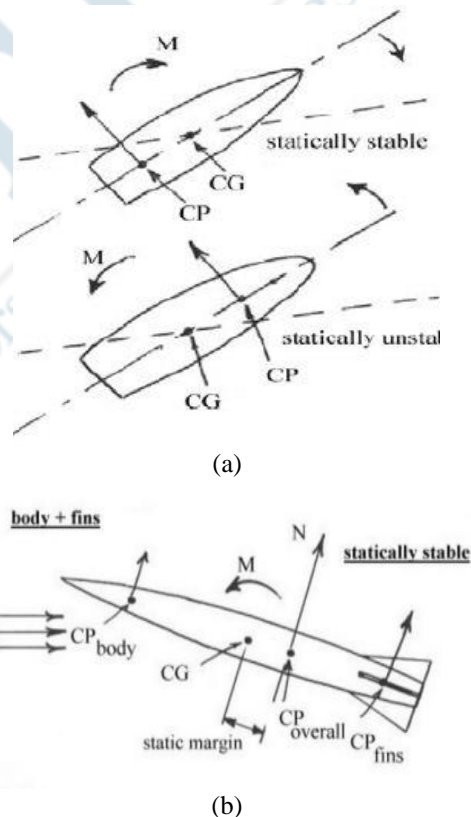

(a)

(b)

Figure 3: (a) Spin Stabilization [25] and (b) Fin Stabilization [26]

3.3 Drag Force, Drag Coefficient (C_D) and Ballistic Coefficient (C)

The drag force is the resistance force imparted on a moving object by a fluid (such as air). In the context of a ballistic trajectory, drag force opposes the projectile's motion and is affected by variables such as the projectile's shape, size,

velocity, and air density. It can considerably affect the projectile's trajectory and accuracy [20]. Moreover, the air drag can have different values, depending on the design of the projectile, that is, muzzle velocity, weight, aerodynamics, and the properties of air, for example, density, temperature, wind, speed of sound. Eqns. (1)-(4) gives the formulae of drag force (F_D), drag coefficient C_D and ballistic coefficient (C).

$$F_D = -\frac{1}{2}\rho S C_D VV = -\frac{1}{2}\rho V^2 s C_D . \vec{I} \qquad (1)$$

A higher ballistic coefficient leads to a flatter trajectory with less drop, enabling the projectile to maintain velocity and energy better over distance. It also reduces the drag force experienced by the projectile, allowing for increased range and accuracy. A projectile's capability to withstand resistance from the air or drag as it moves throughout the air is gauged by its ballistic coefficient. It affects both the trajectory and the magnitude of the drag force experienced by the projectile.

$$C = \frac{m}{d^2} \qquad (2)$$

C_D is determined by friction, pressure, and induced drag, whereas, friction is dependent on the fluid's properties and Reynolds number, while pressure is caused by the pressure difference between the leading and trailing edges. Moreover, induced drag is caused by vortices generated at the blade's point. Also, C_D is directly proportional to the angle of attack. C_D is dependent on several other dimensionless variables. For the general class of projectiles typically used in exterior ballistics, these include the following Mach Number, Reynold's Number, Yaw angle and Various non-dimensional shape parameters, which collectively specify the projectile's shape.

$$C_{D^*} = \frac{\rho S C_D}{2m} = \frac{\rho\pi}{8}\frac{C_D}{C} \qquad (3)$$

$$S = \frac{\pi d^2}{4} \qquad (4)$$

Were, C_D is the drag coefficient; ρ is represented as the air density; V is represented as the velocity of projectile; m is represented as mass and d is represented as d; S is represented as the frontal surface area of the projectile; F_D is the drag force

3.3.1 Mach Number, Reynold Number, Yaw Angle and Various non-dimensional shape parameters

Mach number is given as V/a, whereby V is the characteristic velocity of the bullet and a is the velocity of sound in the medium. It is a parameter without dimensions that gives an indication of the velocity of an object in relation to a sound's frequency. The link among bullet length and drag coefficient is influenced by the Reynolds number. In general, there is little correlation among drag and the Reynolds number. Occasionally when calculating the Reynolds number, the measurement of length, l, is swapped out for the corresponding diameter d. When an aero plane moves to the right, the inclination of yaw among its point of symmetry and

the wind's relative direction is favorable. Fig. 4(a) shows the variation diagram of C_D vs Ma. Fig. 4(b) shows the Sound barrier representation of C_D vs Ma. Eqn. (5) fives the formula representation of Mach number.

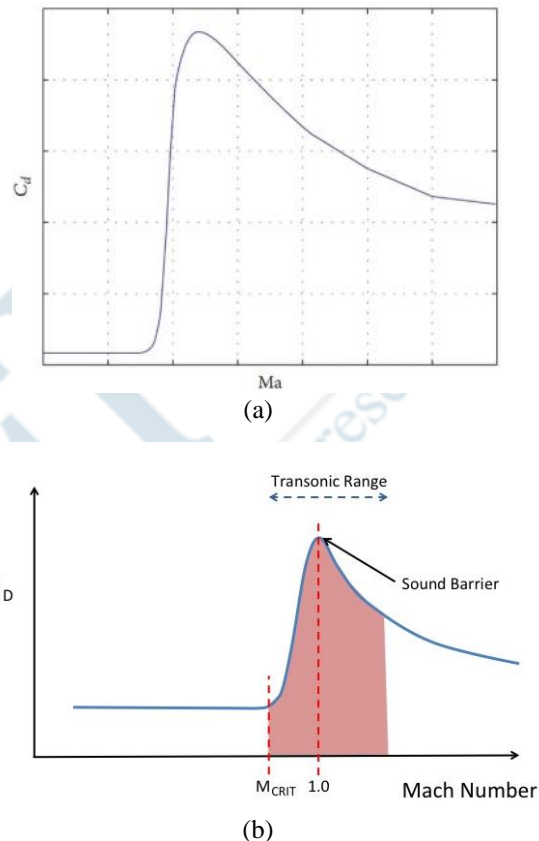$$Ma = \frac{Velocity}{Speed\ of\ sound} \qquad (5)$$

(a)

(b)

Figure 4: (a) Variation graph of C_D vs Ma. [27] and (b) Sound barrier representation of C_D vs Ma [20]

The calculated Mach number represents the ratio of the projectile's velocity to the speed of sound in the medium. Since the coefficient of drag does not vary linearly with Mach number, analytic solutions are inaccurate and difficult to implement. With modern computer capacity, exact solutions are typically approximated or solved numerically by dividing the area under the curve into quadrilaterals and adding their areas. Mach number provides information about the projectile's speed in relation to the sound speed, indicating whether the projectile is:

Subsonic (Mach number < 1): The C_D is constant and consistent through the flying zone of sub-sonic (Ma < 1)

Transonic (Mach number close to 1): The behavior of C_D is complicated and variable in the transonic aviation domain (Ma~1). It is affected by things like waves of shock and modifications in flow patterns. Consequently, the drag coefficient might not have a straightforward connection with the Mach number in the transonic domain.

Supersonic (Mach number > 1): When Ma > 1, which is the low-supersonic region, C_D is inversely related to the square of the root of Mach. C_D declines as Ma rises, though not as quickly as in the extremely high supersonic domain.

Hypersonic (Mach number >> 1): When C_D is inversely correlated to Ma in the extreme ultrasonic flight domain (Ma>>1), indicating that as Ma rises, C_D falls.

3.3.2 Wind Drift

In a missile path, air drifting refers to the lateral divergence of the missile from its original path. A missile must contend with the weight of the wind's strength while in flight. A lateral impact referred to as atmospheric drifting that is created when the wind pressure combines with the projectile's form, speed, and cross-sectional dimension [28]. Fig. 5(a) shows the wind velocity and the projectile's speed in relation to the ground. Fig. 5(b) shows the missile speed in air orientation border. The formulation of wind drift is given in Eqn. (6)

$$x_d = V_w(t_a - t_v) \qquad (6)$$

Were, x_d is represented as the lateral displacement; V_w is represented as the wind velocity; t_v is represented as the projectile's period of flight in a vacuum and t_a is represented as the projectile's flight duration in relation to its destination.
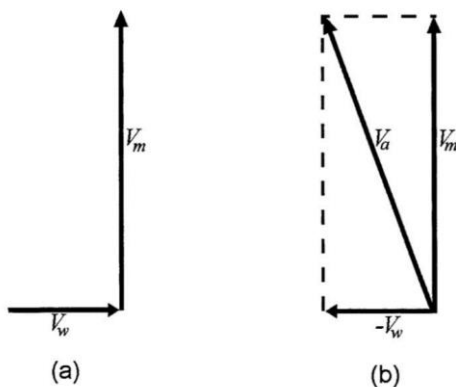

Figure 5: (a) Wind velocity, V_w and projectile velocity, V_m in ground reference frame [28] (b) Projectile velocity in air reference frame [28].

IV. PROJECT METHODOLOGY OF 2 DOF AND 3 DOF MODELS

Two independent papers served as the basis for the study based on point-mass model. The paper by [3] was the foundation for model A (2 DOF Model), while the paper by [4] (3 DOF Model) formed the basis for model B, which incorporated the velocity of the projectile relative to wind velocities. After that efforts were made to replicate their respective models in MATLAB using the ode45 solver. The models described in the papers were replicated in MATLAB, and the ode45 solver was used to solve the resulting equations. The outputs and plots of these models were compared with the published results in the papers to validate

the correctness of the implementations. Once the initial models were validated, modifications were made to incorporate additional effects. This included the consideration of varying drag coefficients based on the Mach number, lateral displacement or drift caused by wind, and the integration of wind effects on the projectile's trajectory. These modifications were based on insights from various publications and relevant studies.

In accordance with the idea of a simpler point-mass mode that was verified by Doppler DR-5000 metrics, a mathematical framework is used for estimating the trajectory's components of a 105 mm axi-symmetric wedge proof shot was developed. This model was created for the creation of suitable range table settings for regular firing. Projectile geometry, air circumstances, gun speed, degree of preference, drag coefficient, and other factors were also considered [3]. The drag difference and flight element estimate of a ultrasonic missile with two dissimilar nose shapes were studied using the simulation's coefficient of drag as an input parameter. The aim was to determine the drag coefficient and shock wave design for a 130-mm weaponry missile (with retrieval plug and fuse) traveling at null angle of occurrence in an ultrasonic movement of air. The simulation's constant of drag was used to estimate trajectory elements, which were validated using chasing detector data from an investigational firing [4]. Fig. (6) shows the workflow diagram of the trajectory.
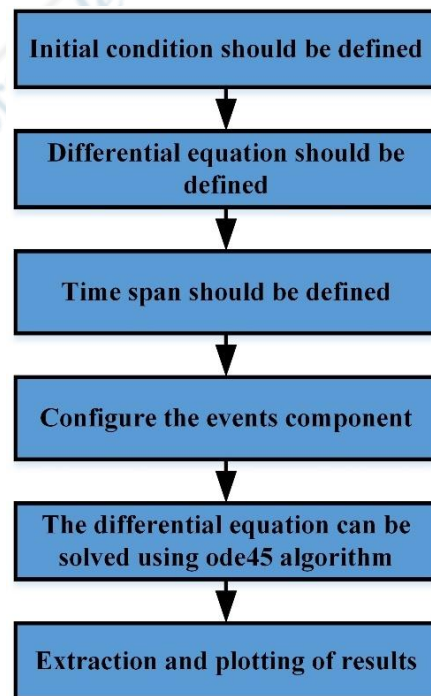

Figure 6: Workflow diagram of the trajectory

4.1. Ballistic Trajectory governing Model A

In Model A, a 2-dimensional simplified point-mass model ($\frac{\rho}{d} < 3$) was considered. Here, the earth is flat and the missile

is in planar motion, with axis that do not roll. Moreover, there is no wind velocity and earth's revolution is disregarded. The drag strength is squarely comparative to the prompt speed. During firing, the drag coefficient and air compactness are presumed to be continuous. The gravitational force remains constant regardless of altitude. Thus, the cross-effects of all forms of forces, including centrifugal, Coriolis, and magnus forces, are insignificant. The drift is comparative to the product of the square of flight time and the cosine of the viewing angle. A simplified point-mass/simple particle trajectory model with three degrees of freedom (3-DOFs) was developed for the purpose of simulating a planar projectile trajectory using mathematical equations. Fig. (7) shows the reference scheme and exterior forces acting on a missile for a characteristic aircraft [4]. Eqn. (7) is based on the missile's speed (V) and the angle at which the angle to the path intersects with the straight line (θ).
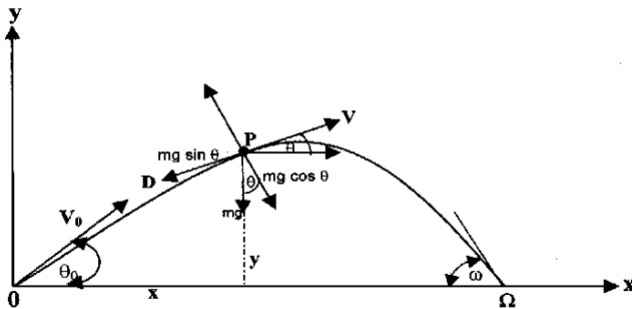

Figure 7: Reference structure and exterior forces acting on a missile for a typical aircraft [3]

$$m \times \frac{dV}{dt} + D + mg \sin \theta = 0$$

$$mV \times d\,\theta/dt + mg \cos \theta = 0$$

$$dx/dt - V \cos \theta = 0$$

$$dy/dt - V \sin \theta = 0 \qquad (7)$$

Were, m is represented as the mass; dV/dt is the rate of change of velocity with respect to time; $d\,\theta/dt$ is represented as the angular velocity (rate of change of angle made with horizontal axis); D is the drag force; g is defined as the acceleration due to gravity; $\frac{dx}{dt}$ and dy/dt is represented as the instantaneous change in position over the instantaneous change in time; V is the velocity.

Moreover, the drag coefficient C_D in D= $\rho S C_D \frac{V^2}{2}$ is projected by Eqn. (8),

$$C_D = C_{D_0} + C_{D_{\alpha^2}} \alpha^2 \qquad (8)$$

$$D_{ft} = K.t^2.\cos\varepsilon \qquad (9)$$

$$\tan = (y/x) \qquad (10)$$

The drift formula is given in Eqn. (9), where the constant K depends on the shape and size of the missile and the value

of C_D can be used as an approximation. At each instant of position *(x, y)* at time *t*, the angle of sight was calculated from Eqn. (10). In this investigation, constant density was assumed during testing to simplify model computation by Eqn. (11).

$$f_1 = \frac{dV}{dt} = -\left(\frac{D}{m}\right) - g \sin \theta$$

$$f_2 = \frac{d\theta}{dt} = -g \cos \theta / \text{V}$$

$$f_3 = \frac{dx}{dt} = V \cos \theta$$

$$f_4 = \frac{dy}{dt} = V \sin \theta \qquad (11)$$

Iterative computations are used to determine the following series of variables using the original values that have been provided. Using the known values each stage's speed, direction, x-position and y-position are adjusted. Once the projectile's y-position turns poor, signaling procedure is continued. Moreover, the variables of $V_{i+1}, x_{i+1}, y_{i+1}$ and θ_{i+1} has been given in every iteration in Eqn. (12). Ode45 solver is used to solve these equations.

$$\Delta V = (-\left(\frac{D}{m}\right) - g \sin \theta)\Delta t$$

$$\Delta \theta = (-g \cos \theta / V)\Delta t$$

$$\Delta x = (V \cos \theta) \Delta t$$

$$\Delta y = (V \sin \theta) \Delta t \qquad (12)$$

For the variable drag coefficient part, in order to make more accurate calculations, the data points were taken from the graph that showed the relationship between the drag coefficient and the Mach number in Robert L. McCoy's book and used a tool in MATLAB called the curve fitting tool to estimate the values between those data points. This process is called interpolation. By doing this, we were able to come up with equations that describe the relationship between the drag coefficient and the Mach number for different speed ranges: subsonic (slower than the speed of sound), transonic (near the speed of sound), and supersonic (faster than the speed of sound).

4.2. Ballistic Trajectory governing Model B

The ballistic trajectory/projectile here is only subject to the effects of gravity and drag in a three-dimensional (3 DOF) model. It is considered a point mass object. Since the overall yaw is minimal together the entire trajectory in this case, both the lift and Magnus pressure are negligible and are not taken into account. Additionally, the earth's curvature and spin are disregarded. Additionally, air density remains consistent along the entire journey. At first, a CFD (Computational Fluid Dynamics) analysis of the projectiles was carried out to find their drag coefficients at various. GAMBIT 2.2 and FLUENT 6.3 were used to numerically simulate a projectile in a ultrasonic stream of air. Shell geometry and meshing were

created using quad element and map type meshing. The drag coefficient values obtained through the mathematical imitations labeled in the preceding sections were utilized as input parameters for modeling the trajectory elements.

Next, to achieve a more precise calculation in the variable drag coefficient modification, the results of the above CFD simulation were used. Specifically, the drag coefficient values for the shell with the fuse projectile as mentioned in the paper, was used. These values were interpolated against the Mach numbers and the curve-fitting toolbox in MATLAB was further used to get the plot and equations for the subsonic, transonic, and supersonic regions

In dynamic firings, the experimental results provided by tracking radar were used to validate the imitation results. The origin of this coordinate system is the cannon muzzle. The X-axis is focused towards the target from the rifle. Through the launch point, the Y-axis is focused upward vertically. Looking downrange, the Z-axis is aligned to the right. Fig. (8) shows the 3-D Coordinate System for point-mass trajectory. The subsequent equations of motion for each of the three axes can be determined employing Newton's second law in Eqn. (13). For computing reasons, the complex equations from the preceding presentation can now be simplified to this vector form in Eqn. (14),

$$\frac{dV_x}{dt} = -\frac{\rho S C_D}{2m} V V_x$$

$$\frac{dV_y}{dt} = -\frac{\rho S C_D}{2m} V V_y - g$$

$$\frac{dV_z}{dt} = -\frac{\rho S C_D}{2m} V V_z \tag{13}$$

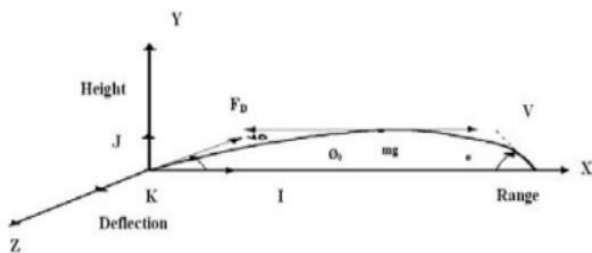$$V = \sqrt{V_x^2 + V_y^2 + V_z^2} \tag{14}$$

Figure 8: 3-D Coordinate System for point-mass trajectory [4]

The formulas for the equations for motion is given in Eqn. (15) have been recalculated by the tail wind (which in turn positive when blown from the firearm towards the intended aim W_x, positive when blown upwards vertically W_y, and positive when blown from left to right crossing the line of fire W_z) in the following manner [4] and [20].

$$\frac{dV_x}{dt}$$
$$= -\frac{\rho S C_D}{2m}\left\{\sqrt{(V_x - W_x)^2 + (V_y - W_y)^2 + (V_z - W_z)^2}\right\}(V_x - W_x)$$

$$\frac{dV_y}{dt}$$
$$= -\frac{\rho S C_D}{2m}\left\{\sqrt{(V_x - W_x)^2 + (V_y - W_y)^2 + (V_z - W_z)^2}\right\}(V_y - W_y) - g$$

$$\frac{dV_z}{dt} =$$
$$-\frac{\rho S C_D}{2m}\left\{\sqrt{(V_x - W_x)^2 + (V_y - W_y)^2 + (V_z - W_z)^2}\right\}(V_z - W_z) \tag{15}$$

Moreover, the numerical simulation was then used to determine the trajectory's components, including the terminal V_x, terminal V_y, X-distance (range), Y-distance (height) and the duration of flight and the input parameters that is given in Tab. (1) and it shows the input parameters and its values,

- Initial (muzzle) velocity = V_o,
- Initial X-direction velocity $V_x = V_o \cos\theta$,
- Initial Y-direction velocity $V_y = V_o \sin\theta$,
- Initial coefficient of drag = C_{D_o},
- Initial X-distance (range) = 0,
- Initial Y-distance (height) = 0,
- Initial elevation = θ_o and, initial time (t) = 0

Table 1: Input Parameters [4]

Parameters	Numerical Values
Mass of the projectile	33.4 kg
Diameter of projectile	0.13 m
Angle of elevation	7.5°
Wind velocity	0

4.3. ODE45 Solver in MATLAB

Ordinary differential equation (ODE) equations are frequently solved using ODE45, a computerized processor in MATLAB's ODE package. It uses dynamic time-stepping and a fourth- and fifth-order Runge-Kutta equation to strike a compromise among precision and efficiency [29]. Some steps of Ode45 is given below,

1. **Variable-Step Method:** ODE45 employs a dynamic time-stepping method, which means that while unity, the step size is changed on the fly.
2. **Fourth and Fifth-Order Formulas:** Runge-Kutta formulas of fourth and fifth orders are combined in ODE45 to determine the answer.
3. **Dense Output:** ODE45 generates packed results, it can calculate the answer at any arbitrary location

along its integration period.

4. **Non-Stiff Problems:** When the solution to a problem fluctuates gradually over a period of time and doesn't show sudden shifts or abrupt changes, ODE45 is a good fit.

5. **Limited Efficiency for Stiff Problems:** ODE45 is capable of handling issues with modest stiffness, but it might not be the best option for situations with excessive stiffness.

V. RESULTS AND DISCUSSIONS

The goal of this work was to use a computational method using MATLAB simulation software to analyze a projectile's aerodynamic flight parameters. In order to precisely anticipate the path of the bullet under various circumstances, the simulation entailed the application of mathematical frameworks and techniques. The outcomes of the simulation conducted in MATLAB offered insightful information about several facets of the ballistic trajectory. Additionally, the modeling process gave us the opportunity to examine how resistance to air affected the trajectory of the bullet. In comparison to the perfect scenario lacking resistance to air it is founded that the projectile's highest point and distance were reduced when the resistance of air was accounted for in the simulation.

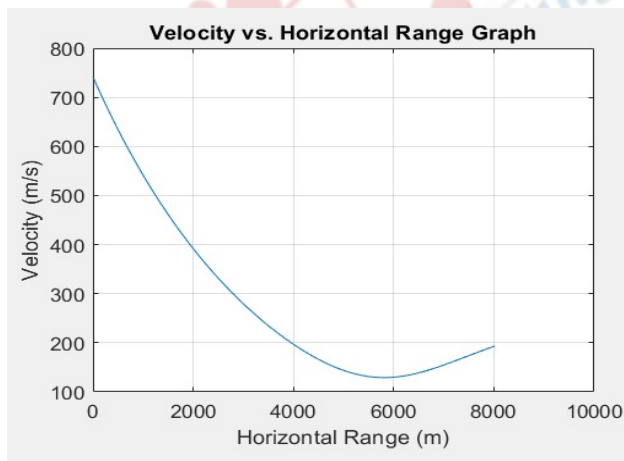### 5.1 Trajectory Model A with constant drag coefficient

The graphs that follow compare the results presented in the manner of graphs and values for outputs among the initial model reported in the research by [3] and the produced adaption of the framework (A.). The comparison values from the created component and the initial publication are displayed in Tab. (2) and Tab. (3) shows the percentage accuracy of the compared values and Fig. 9(a) shows the diagram of velocity vs horizontal range plot and (b) shows the diagram of velocity vs horizontal range plot generated according to the present study with constant drag coefficient.

**Table 2:** Generated values comparison with the values present in the original paper [3]

Muzzle Velocity (m/s)	Initial angle of elevation (θ^o)	Time of flight (s)		Range (m)		Drift (m)	
		Original paper values	Generated values	Original paper values	Generated values	Original paper values	Generated values
741.60	45.0	53.06	52.94	7997.32	8108.4	1406.54	1390.34
747.30	30.0	40.73	40.55	8511.56	8631.3	0829.08	0810.76

Table 3: Percentage accuracy of the compared values

| Muzzle Velocity (m/s)	Initial angle of elevation (θ^o)	Accuracy (%)		
		Time of Flight	Range	Drift
741.60	45.0	-0.226	+1.388	-1.15
747.30	30.0	-0.441	+1.407	-2.20
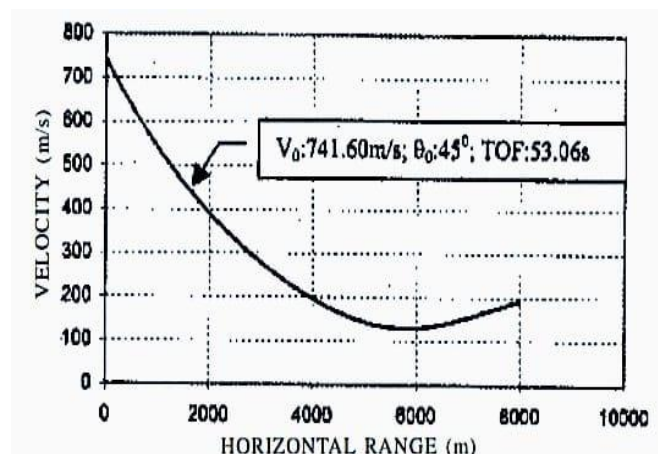
(a)	(b)

Figure 9: (a) velocity vs horizontal range plot [3] (b) velocity vs horizontal range plot generated according to the present study with constant drag coefficient [3]

5.1.1. *Trajectory Model A with variable drag coefficient*

By taking into account the changes in drag coefficient with velocity, the subtle variations in drag force that occur at different speeds can be captured. This finer level of precision can lead to more accurate predictions, especially when dealing with high-velocity projectiles or situations where the velocity varies significantly. It's worth noting that while the variable C_D model may provide a more accurate picture, it still requires validation against experimental findings to establish its reliability and accuracy. The availability of experimental data is crucial for validating and refining simulation models, allowing for more confident predictions in real-world scenarios. Fig. (10) shows the velocity vs horizontal range graph.
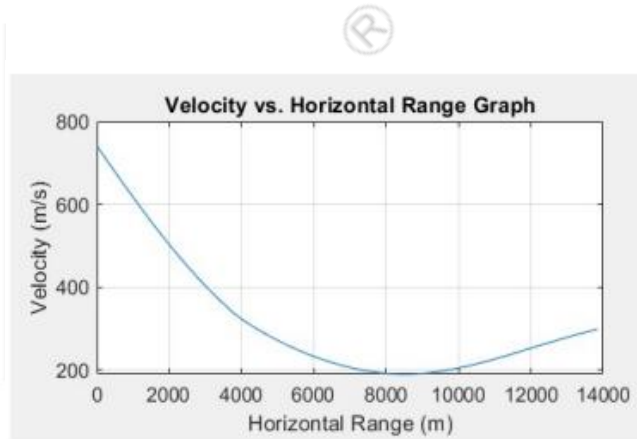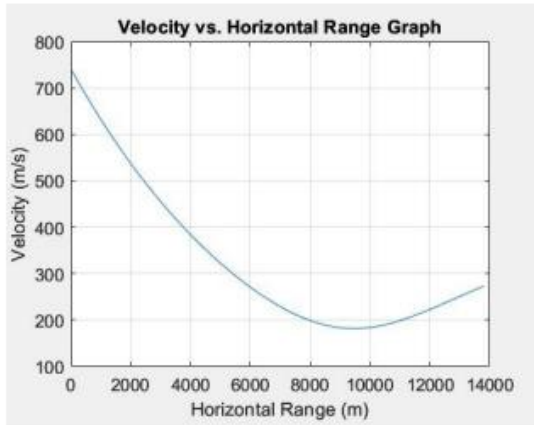
(a.) Velocity versus Range (constant C_D)   **(b.) Velocity versus Range (variable C_D)**

Figure 10: Velocity versus Horizontal range graph

5.1.2. *Trajectory Model B with constant drag coefficient*

Similar to the values of model A in Tab. 2 and 3, it is clearly evident that the outputs of the two simulations the original plots and the plots generated in this code using the same parameters are similar with not much difference in the values. Thus, this validates our mathematical model and simulation method. Tab. (4) gives the generated values comparison with the values present in the original paper along with percentage error between the simulated and experimental values. Fig. 11 (a) shows the plot for X distance and X velocity graph published in the paper and (b) shows the generated graph for X distance and X velocity graph for a constant drag coefficient.

Table 4: Generated values comparison with the values present in the original paper along with percentage error between the simulated and experimental values [4]

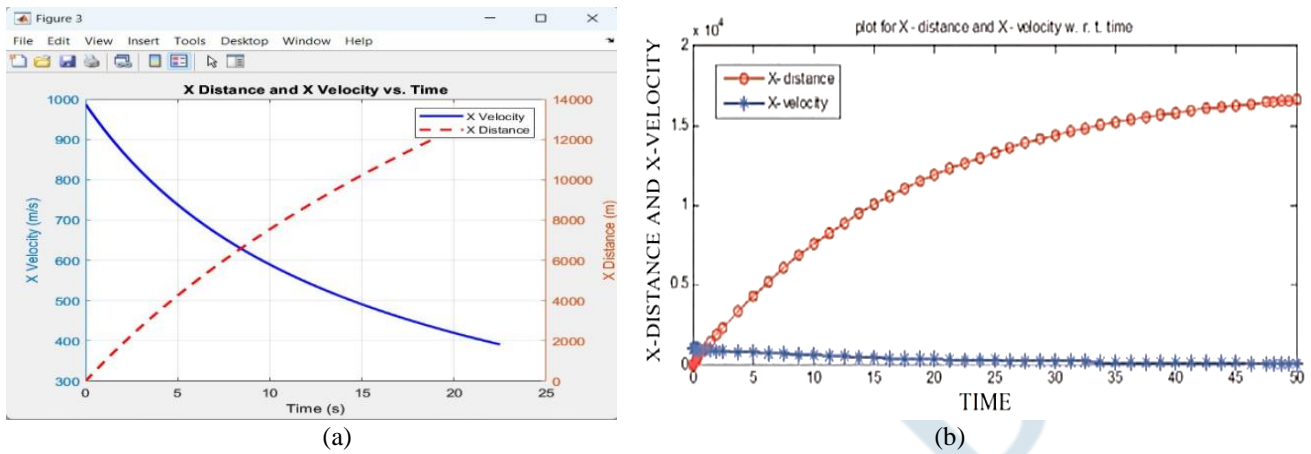| Velocity(m/s) (Shell with Fuse)		Simulated Result (reference paper (I)	Present Simulated Result (II)	Experimental Results (III)	Error (%) between (III) and (I)	Error (%) between (III) and (II)
	C_D	**0.2297**	**0.31**	**0.31**		
996.1	Range (km)	12.48	13.02	13.36	-6.58	-2.54
	Time of Flight (s)	22.09	21.49	22.20	-0.49	-3.19
	C_D	**0.2306**	**0.28**	**0.28**		
1003.1	Range (km)	12.68	13.68	13.51	-6.14	+1.25
	Time of Flight (s)	22.20	21.75	22.05	+0.68	-1.36

(a) (b)

Figure 11: (a)Plot for X distance and X velocity graph published in the paper [4] (b)Generated graph for X distance and X velocity graph [4].

5.1.3. *Trajectory Model B with varying drag coefficient*

Tab. (5) gives the generated values comparison with the values present in the original paper along with percentage error between the simulated and experimental values. Fig. 12 (a) shows the plot for Y distance and Y velocity graph published in the paper and (b) shows the generated graph for Y distance and Y velocity graph for varying drag coefficient.

Table 5: Generated values (variable C_D) comparison with the values present in the original paper along with percentage error between the simulated and experimental values [4]

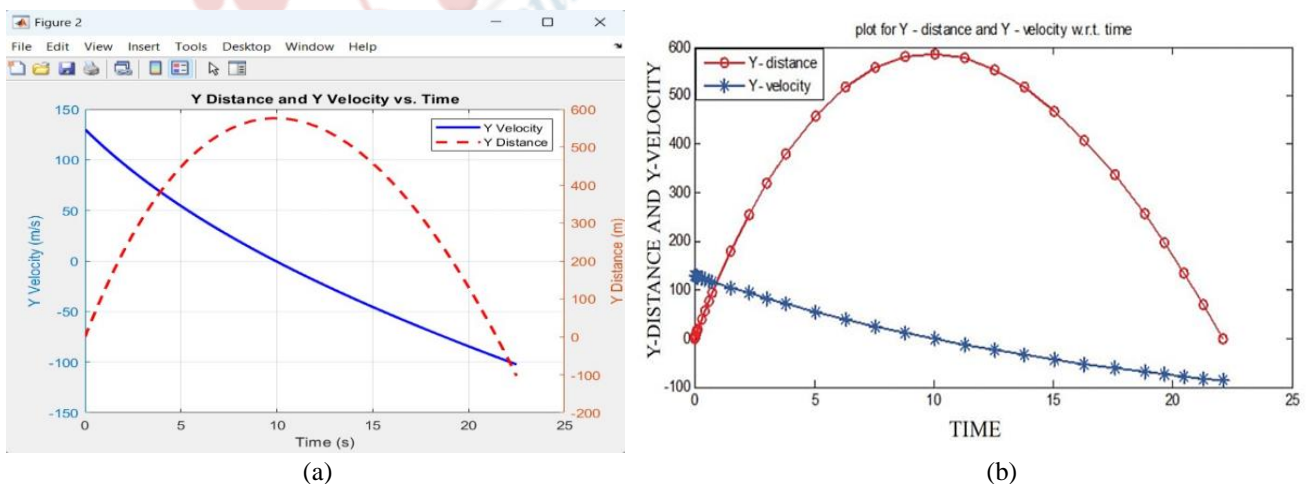| Velocity(m/s) (Shell with Fuse)		Simulated Result (reference paper (I)	Present Simulated Result (II)	Experimental Results (Taken from reference paper (III)	Error (%) between (III) and (I)	Error (%) between (III) and (II)
996.1	**Range (km)**	12.48	13.32	13.36	-6.58	-0.299
	Time of Flight (s)	22.09	22.09	22.20	-0.49	-0.49
1003.1	**Range (km)**	12.68	13.51	13.51	-6.14	0
	Time of Flight (s)	22.20	22.18	22.05	+0.68	+0.58

(a) (b)

Figure 12: (a)Plot for Y distance and Y velocity graph published in the paper [4] (b)Generated graph for Y distance and Y velocity graph [4].

5.2 Discussions

In Fig. (1) it shows the diagram of typical ballistic trajectory. Fig. (2) shows the diagram of 6 DOF motion. Fig. 3(a) and (b) shows the spin and fin stabilization of the projectile. Fig. 4(a) shows the variation diagram of C_D vs Ma. Fig. 4(b) shows the Sound barrier representation of C_D vs Ma. Fig. 5(a) shows the wind velocity and missile speed in ground reference frame, Fig. 5(b) shows the missile speed in air reference frame. Fig. (6) shows the workflow diagram of the trajectory. Fig. (7) shows the reference structure and exterior forces acting on a projectile for a typical flight. Fig. (8) shows the 3-D Coordinate System for point-mass trajectory. Tab. (1) shows the input parameters of the projectile. The comparison values from the created component and the initial publication are displayed in Tab. (2) and Tab. (3) shows the percentage accuracy of the compared values. Fig. 9(a) shows the diagram of velocity vs horizontal range plot and (b) shows the diagram of velocity vs horizontal range plot generated according to the present study with constant drag coefficient. Fig. (10) shows the velocity vs horizontal range graph. Tab. (4) gives the generated values comparison with the values present in the original paper along with percentage error between the simulated and experimental values. Fig. 11 (a) shows the plot for X distance and X velocity graph published in the paper and (b) shows the generated graph for X distance and X velocity graph. Tab. (5) gives the generated values contrast with the values present in the original paper along with percentage error between the simulated and experimental values. Fig. 12 (a) shows the plot for Y distance and Y velocity graph published in the paper and (b) shows the generated graph for Y distance and Y velocity graph.

VI. CONCLUSION AND FUTURE SCOPE

The results obtained from the simulations and analysis support the validation of the mathematical model and simulation method used in this study. Comparing the plots and output values between the original simulations and the ones generated in this code using the same parameters demonstrates that there is a minimal difference, thus confirming the accuracy of the model. Results from simulations and analysis support the validation of the mathematical model and simulation method used in this study. Plots and output values from the original simulations and the ones generated in this code show minimal differences, confirming the accuracy of the model. Reducing the simulation's time span (tspan) can improve the precision of matching between the original and generated values. Adjusting tspan to a range closer to the anticipated flight duration allows the simulation to focus on the specific time interval of interest, leading to a more accurate correlation with the published paper. A balance must be struck between precision and capturing the entire projectile behavior, as excessively reducing the span may cut off the trajectory or omit important dynamics. The modified version of model A, which considers drift and lateral displacement due to a constant crosswind and incorporates a variable drag coefficient based on Mach number, shows promising results. The variable drag coefficient captures subtle variations in drag force at different velocities, particularly beneficial for high-velocity projectiles or scenarios with significant velocity fluctuations. Experimental validation is necessary to establish the reliability and accuracy of the variable drag coefficient model. The evaluation between the constant C_D model and the variable C_D model in Model B indicates that the latter yields better agreement between simulated and experimental values. The varying drag coefficient based on Mach number provides a more realistic representation of the system, reflecting changing flow regimes. Emphasizes the non-constant nature of the drag coefficient, which varies with the velocity of the object. With the goal to increase the reliability as well as precision of the models used for simulation, it is crucial to conduct actual evaluations and measurements to confirm the data gathered. Moreover, the simulations have a solid basis that may be built upon when the values generated by simulation are contrasted to the real data collected from experiments.

REFERENCES

[1] D. Klatt, M. Proff, and R. Hruschka, "Investigation of the flight behavior of a flare-stabilized projectile using 6DoF simulations coupled with CFD," *Int. J. Numer. Methods Heat Fluid Flow*, vol. 30, no. 9, pp. 4185–4201, Jun. 2019, doi: 10.1108/HFF-05-2018-0217.

[2] C. Tola, P. Beyazpinar, and D. Akin, "Analysis of Range Extension Process for Outdated Ballistic Munitions Ejected from an Accelerator Launcher Concept," *J. Aviat.*, vol. 5, no. 2, pp. 90–100, Dec. 2021, doi: 10.30518/jav.974811.

[3] K. K. Chand and H. S. Panda, "Mathematical Model to Simulate the Trajectory Elements ofan Artillery Projectile Proof Shot," *Def. Sci. J.*, vol. 57, no. 1, pp. 139–148, Jan. 2007, doi: 10.14429/dsj.57.1741.

[4] S. Sahoo and M.K. Laha, "Coefficient of Drag and Trajectory Simulation of 130 mm Supersonic Artillery Shell with Recovery Plug or Fuze," *Def. Sci. J.*, vol. 64, no. 6, pp. 502–508, Nov. 2014, doi: 10.14429/dsj.64.8110.

[5] K. P. Meena and S. Sharma, "Applications of Projectile Motion in Real Life and Technological Advancements," *Cent. Asian Stud.*, vol. 03, no. 11, 2022.

[6] B. Parate, Y. Salkar, S. Chandel, and H. Shekhar, "A Novel Method for Dynamic Pressure and Velocity Measurement Related to a Power Cartridge Using a Velocity Test Rig for Water-Jet Disruptor Applications," *Cent. Eur. J. Energ. Mater.*, vol. 16, no. 3, pp. 319–342, Jul. 2019, doi: 10.22211/cejem/110365.

[7] J. Zhang, S. Yu, and Y. Yan, "Fixed-time output feedback trajectory tracking control of marine surface vessels subject to unknown external disturbances and uncertainties," *ISA Trans.*, vol. 93, pp. 145–155, Oct. 2019, doi: 10.1016/j.isatra.2019.03.007.

[8] L. Kaňáková, J. Mazáčková, V. Nosek, and P. Huta, "External and Terminal Ballistics of Early Bronze Age Lithic Arrowheads: Experimental Verification," *Lithic Technol.*, vol. 47, no. 3, pp. 266–281, Jul. 2022, doi: 10.1080/01977261. 2022.2040139.

[9] D. Horla, "Variational Calculus Approach to Optimal Interception Task of a Ballistic Missile in 1D and 2D Cases," *Algorithms*, vol. 12, no. 8, p. 148, Jul. 2019, doi: 10.3390/ a12080148.

[10] J. Chinnasamy *et al.*, "Study and Simulation of Autonomous Quadrotor Tracking a Pre-Defined Trajectory Using Matlab," *IOP Conf. Ser. Mater. Sci. Eng.*, vol. 1055, no. 1, p. 012045, Feb. 2021, doi: 10.1088/1757-899X/1055/1/012045.

[11] M. Jahangir, S. T. Iqbal, S. Shahid, I. A. Siddiqui, and I. Ulfat, "MATLAB Simulation for Teaching Projectile Motion," *Adv. J. Sci. Eng.*, vol. 1, no. 2, pp. 59–61, Jun. 2020, doi: 10.22034/ AJSE.2012059.

[12] M. J. Koushik, M. S. A. Krishna, R. Rahul, and P. Sreedharan, "Foot trajectory analysis of a robotic leg," *J. Phys. Conf. Ser.*, vol. 2070, no. 1, p. 012172, Nov. 2021, doi: 10.1088/1742-6596/2070/1/012172.

[13] R. Głębocki and M. Jacewicz, "Parametric Study of Guidance of a 160-mm Projectile Steered with Lateral Thrusters," *Aerospace*, vol. 7, no. 5, p. 61, May 2020, doi: 10.3390/ aerospace7050061.

[14] Y. Xu, Z. Zhijun Wang, and F. Dong, "Ballistic Trajectory Modeling for Missile with Deflectable Nose," *Mechanics*, vol. 26, no. 5, pp. 450–456, Oct. 2020, doi: 10.5755/j01. mech.26.5.27874.

[15] N. Moshtaghi Yazdani and M. H. Olyaei, "Optimization of Electromagnetic Railgun and Projectile's Trajectory by Genetic Algorithm," *Majlesi J. Telecommun. Devices*, vol. 11, no. 1, pp. 27–32, Mar. 2022, doi: 10.52547/mjtd.11.1.27.

[16] S. A. El-Hakem Hegazy, A. M. Kamel, I. I. Arafa, and Y. Z. Elhalwagy, "INS Stochastic Noise Impact on Circular Error Probability of Ballistic Missiles," *Navig. J. Inst. Navig.*, vol. 69, no. 2, p. navi.523, 2022, doi: 10.33012/navi.523.

[17] M. Jacewicz, P. Lichota, D. Miedziński, and R. Głębocki, "Study of Model Uncertainties Influence on the Impact Point Dispersion for a Gasodynamicaly Controlled Projectile," *Sensors*, vol. 22, no. 9, p. 3257, Apr. 2022, doi: 10.3390/s2209 3257.

[18] C. A. Rabbath and D. Corriveau, "A comparison of piecewise cubic Hermite interpolating polynomials, cubic splines and piecewise linear functions for the approximation of projectile aerodynamics," *Def. Technol.*, vol. 15, no. 5, pp. 741–757, Oct. 2019, doi: 10.1016/j.dt.2019.07.016.

[19] J. Stearns and G. Moddel, "Simulation of Z-Shaped Graphene Geometric Diodes Using Particle-in-Cell Monte Carlo Method in the Quasi-Ballistic Regime," *Nanomaterials*, vol. 11, no. 9, p. 2361, Sep. 2021, doi: 10.3390/nano11092361.

[20] R. McCoy, *Modern exterior ballistics: The launch and flight dynamics of symmetric projectiles*. Schiffer Pub., 1999.

[21] G. D. Di Martino, C. Carmicino, S. Mungiguerra, and R. Savino, "The Application of Computational Thermo-Fluid-Dynamics to the Simulation of Hybrid Rocket Internal Ballistics with Classical or Liquefying Fuels: A Review," *Aerospace*, vol. 6, no. 5, p. 56, May 2019, doi: 10.3390/ aerospace6050056.

[22] A. Milks, D. Parker, and M. Pope, "External ballistics of Pleistocene hand-thrown spears: experimental performance data and implications for human evolution," *Sci. Rep.*, vol. 9, no. 1, p. 820, Jan. 2019, doi: 10.1038/s41598-018-37904-w.

[23] L. Sentry Admin, "Lone Sentry Blog | World War II Photographs, Documents, and Research," 2020. https://www. lonesentry.com/blog/ (accessed Jun. 24, 2023).

[24] Tom Benson, "Rocket Rotations," 2021. https://www.grc. nasa.gov/www/k-12/rocket/rotations.html (accessed Jun. 22, 2023).

[25] L. Baranowski, "Equations of motion of a spin-stabilized projectile for flight stability testing," *J. Theor. Appl. Mech.*, vol. 51, no. 1, pp. 235–246, 2013.

[26] H. L. Zayed, "COMPUTER AIDED AIMING SYSTEM FOR UNGUIDED PROJECTILE FIRING WEAPONS," 2015.

[27] A. Ramezani and H. Rothe, "Simulation-Based Early Prediction of Rocket, Artillery, and Mortar Trajectories and Real-Time Optimization for Counter-RAM Systems," *Math. Probl. Eng.*, vol. 2017, pp. 1–8, 2017, doi: 10.1155/2017/ 8157319.

[28] H. A. Leupold, "Wind Drift of Projectiles: A Ballistics Tutorial.," ARMY RESEARCH LAB FORT MONMOUTH NJ, 1996.

[29] J. V. Vidal, P. Rolo, P. M. R. Carneiro, I. Peres, A. L. Kholkin, and M. P. Soares Dos Santos, "Automated electromagnetic generator with self-adaptive structure by coil switching," *Appl. Energy*, vol. 325, p. 119802, Nov. 2022, doi: 10.1016/j. apenergy.2022.119802.